Grasp Constraint Satisfaction for Object Manipulation using Robotic Hands

Wenceslao Shaw-Cortez, Denny Oetomo, Chris Manzie, and Peter Choong

***Abstract*— For successful object manipulation with robotic hands, it is important to ensure that the object remains in the grasp at all times. In addition to grasp constraints associated with slipping and singular hand configurations, excessive rolling is an important grasp concern where the contact points roll off of the fingertip surface. Related literature focus only on a subset of grasp constraints, or assume grasp constraint satisfaction without providing guarantees of such a claim. In this paper, we propose a control approach that systematically handles all grasp constraints. The proposed controller ensures that the object does not slip, joints do not exceed joint angle constraints (e.g. reach singular configurations), and the contact points remain in the fingertip workspace. The proposed controller accepts a nominal manipulation control, and ensures the grasping constraints are satisfied to support the assumptions made in the literature. Simulation results validate the proposed approach.**

I. Introduction

A primary objective of robotic hand research is to manipulate the environment to achieve a desired goal [1]. This can be accomplished in a hierarchical grasp framework where a high-level planner plans the grasp, forms the grasp, and manipulates the object [2], [3]. The focus of this work is in the manipulation aspect of the hierarchical approach, which consists of rotating/translating the object within the grasp, and hereafter is referred to as in-hand manipulation. In-hand manipulation controllers are used to track a desired object reference trajectory, while keeping the object inside the grasp [4]. Thus for successful in-hand manipulation, it is paramount to guarantee that the object remains in the grasp during the manipulation motion.

A failed grasp can result from slipping, joint over-extension, and excessive rolling. Slipping is an obvious grasping concern, which has been formulated as a constraint satisfaction problem and extensively addressed in the literature [5]–[7]. Joint over-extension relates to joints exceeding feasible joint angle constraints (e.g joint workspace, hardware capabilities, singular hand configurations), which inhibits the robotic hand from applying necessary contact forces to prevent grasp failure [8]. Excessive rolling, as defined here, is when the contact points roll off of the fingertip surface. In-hand manipulation inherently relies on rolling motion for object manipulation. [9]. However excessive rolling motion may cause the contact points to leave the fingertip surface. When this occurs, the contact point violates the workspace constraint of the fingertip resulting in loss of contact. For successful manipulation, the manipulation controller must guarantee grasp constraint satisfaction such that the contact points remain in the fingertip workspace, whilst simultaneously ensuring no slip and no over-extension.

To date, there exist an abundance of multi-fingered robotic hands, including tactile sensors, along with methods of controlling them [4], [10]. However, many manipulation controllers focus on the object manipulation task and assume grasp constraint satisfaction, but provide no guarantees to support that assumption [11], [12]. Other methods focus on one grasp constraint, such as no slipping, but do not systematically consider all grasp constraints [6], [7]. Existing methods of addressing grasping constraints are via motion planning approaches [13]–[15], however they rely on quasi-static assumptions that generally do not hold in a dynamic manipulation setting. Furthermore those approaches require large computational resources and are not conducive to real-time applications [13]. In the hierarchical grasp framework, it is difficult to determine a priori the region of attraction of the in-hand manipulation controller as it depends on both the object and initial grasp configuration. Therefore a given reference trajectory from the high-level planner may result in grasp constraint violation and thus grasp failure. There is no existing method to prevent excessive rolling, no slip, and over-extension for real-time object manipulation.

In this paper, we present a novel controller that systematically handles no slipping, over-extension, and excessive rolling constraints for object manipulation. The proposed controller admits a nominal manipulation control, as found in the literature [4], and outputs a minimally close, in the 2-norm sense, manipulation control torque, while adhering to the grasping constraints. The effectiveness of the proposed controller is validated in simulation.

Notation

Throughout this paper, an indexed vector $\boldsymbol{v}_i \in \mathbb{R}^p$ has an associated concatenated vector $\boldsymbol{v} \in \mathbb{R}^{pn}$, where the index i is specifically used to index over the n contact points in the grasp. The notation $\boldsymbol{v}^{\mathcal{F}}$ indicates that the vector $\boldsymbol{v}$ is written with respect to a frame $\mathcal{F}$, and if there is no explicit frame defined, $\boldsymbol{v}$ is written with respect to the inertial frame, $\mathcal{P}$. The operator $(\cdot)\times$ denotes the skew-symmetric matrix representation of the cross-product. The $k \times k$ identity matrix is denoted $I_{k\times k}$.

W. Shaw-Cortez, D. Oetomo, and C. Manzie are with the MIDAS Laboratory in the School of Electrical, Mechanical, and Infrastructure Engineering, University of Melbourne, 3010, Australia, shaww@student.unimelb.edu.au, doetomo@unimelb.edu.au, manziec@unimelb.edu.au.

P. Choong is with the Department of Surgery, St. Vincent's Hospital, 3065, Australia, pchoong@unimelb.edu.au.

II. Background

A. Hand-Object System

Consider a fully-actuated, multi-fingered hand grasping a rigid, convex object at $n \in \mathbb{Z}_{>0}$ contact points. Each finger consists of $m_i \in \mathbb{Z}_{>0}$ joints with smooth, convex fingertips of high stiffness. Let the finger joint configuration be described by the joint angles, $\boldsymbol{q}_i \in \mathbb{R}^{m_i}$. The full hand configuration is defined by the joint angle vector, $\boldsymbol{q} = (\boldsymbol{q}_1, \boldsymbol{q}_2, ..., \boldsymbol{q}_n)^T \in \mathbb{R}^m$, where $m = \sum_{i=1}^{n} m_i$ is the total number of joints. Let the inertial frame, $\mathcal{P}$, be fixed on the palm of the hand, and a fingertip frame, $\mathcal{F}_i$, fixed at the point $\boldsymbol{p}_{f_i} \in \mathbb{R}^3$. The translational and rotational velocities of $\mathcal{F}_i$ with respect to $\mathcal{P}$ are denoted $\boldsymbol{v}_{f_i}, \boldsymbol{\omega}_{f_i} \in \mathbb{R}^3$, respectively. The contact frame, $\mathcal{C}_i$, is located at the contact point, $\boldsymbol{p}_{c_i} \in \mathbb{R}^3$. A visual representation of the contact geometry for the ith finger is shown in Figure 1.

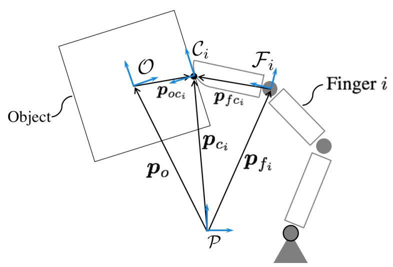

Fig. 1: A visual representation of the contact geometry for contact i.

Let $\mathcal{O}$ be a reference frame fixed at the object center of mass $\boldsymbol{p}_o \in \mathbb{R}^3$, and $R_{po} \in SO(3)$ is the rotation matrix, which maps from $\mathcal{O}$ to $\mathcal{P}$. The respective inertial translation and rotational velocities of the object are $\boldsymbol{v}_o, \boldsymbol{\omega}_o \in \mathbb{R}^3$. The object state is $\boldsymbol{x}_o \in \mathbb{R}^6$, with $\dot{\boldsymbol{x}}_o = (\boldsymbol{v}_o, \boldsymbol{\omega}_o)$. The position vector from $\mathcal{O}$ to the respective contact point is $\boldsymbol{p}_{oc_i} \in \mathbb{R}^3$.

The hand/object dynamics are respectively defined as [8]:

$$M_h \ddot{\boldsymbol{q}} + C_h \dot{\boldsymbol{q}} = -J_h^T \boldsymbol{f}_c + \boldsymbol{\tau}_e + \boldsymbol{u} \tag{1}$$

$$M_o \ddot{\boldsymbol{x}}_o + C_o \dot{\boldsymbol{x}}_o = G \boldsymbol{f}_c + \boldsymbol{w}_e \tag{2}$$

where $M_h := M_h(\boldsymbol{q}) \in \mathbb{R}^{m \times m}, M_o := M_o(\boldsymbol{x}_o) \in \mathbb{R}^{6 \times 6}$ are the respective hand and object inertia matrices, $C_h := C_h(\boldsymbol{q}, \dot{\boldsymbol{q}}) \in \mathbb{R}^{m \times m}, C_o := C_o(\boldsymbol{x}_o, \dot{\boldsymbol{x}}_o) \in \mathbb{R}^{6 \times 6}$ are the respective hand and object Coriolis and centrifugal matrices, $\boldsymbol{\tau}_e := \boldsymbol{\tau}_e(t) \in \mathbb{R}^m$ is the disturbance torque acting on the joints, $\boldsymbol{w}_e := \boldsymbol{w}_e(t) \in \mathbb{R}^6$ is an external wrench disturbing the object, and $\boldsymbol{u} \in \mathbb{R}^m$ is the joint torque control input for a fully-actuated hand. The grasp map, $G := G(\boldsymbol{p}_{oc}) \in \mathbb{R}^{6 \times 3n}$ maps the contact force, $\boldsymbol{f}_c$, to the net wrench acting on the object. The hand Jacobian, $J_h := J_h(\boldsymbol{q}, \boldsymbol{p}_{fc}) \in \mathbb{R}^{3n \times m}$, relates the motion of the hand and velocity of the contact points. The hand Jacobian is a block diagonal matrix of the individual hand Jacobian matrices:

$$J_{h_i}(\boldsymbol{q}_i, \boldsymbol{p}_{fc_i}) = \begin{bmatrix} I_{3\times 3} & -(\boldsymbol{p}_{fc_i})\times \end{bmatrix} J_{s_i}(\boldsymbol{q}_i) \tag{3}$$

where $J_{s_i}(\boldsymbol{q}_i) \in \mathbb{R}^{6 \times mi}$ is the spatial manipulator Jacobian that maps $\dot{\boldsymbol{q}}_i \mapsto (\boldsymbol{v}_{f_i}, \boldsymbol{\omega}_{f_i})$ [8].

When the contact points do not slip, the following grasp constraint holds [16]:

$$J_h \dot{\boldsymbol{q}} = G^T \dot{\boldsymbol{x}}_o \tag{4}$$

The following assumptions are made for the grasp:

Assumption 1. *The multi-fingered hand has $m = 3n$ joints.*

Assumption 2. *The given multi-fingered grasp has $n > 2$ contact points, which are non-collinear.*

Assumption 3. *The local fingertip and object contact surfaces are smooth.*

Remark 1. *Assumption 1 ensures J_h is square, which is a common assumption in related work [6], [11], [12], and can be relaxed by considering internal motion of the dynamics [8]. Assumption 2 ensures G is always full rank [16], and can be ensured by a high-level grasp planner [2].*

B. Hand-Contact Kinematics

Here we review the differential geometric modeling of rolling contacts as presented in [8]. Note, the subscript o will refer to the object surface of the contact, and the subscript f refers to the fingertip surface of the contact. At each contact point, we parameterize the contact surfaces by local coordinates $\boldsymbol{\xi}_{o_i} = (a_{o_i}, b_{o_i}), \boldsymbol{\xi}_{f_i} = (a_{f_i}, b_{f_i})$. The relation between the local coordinates and contact position vectors are defined by smooth mappings: $\boldsymbol{p}_{fc_i} = \boldsymbol{c}_{f_i}(\boldsymbol{\xi}_{f_i}), \boldsymbol{p}_{oc_i} = \boldsymbol{c}_{o_i}(\boldsymbol{\xi}_{o_i})$. The angle between $\frac{\partial \boldsymbol{c}_{o_i}}{\partial a_{o_i}}$ and $\frac{\partial \boldsymbol{c}_{f_i}}{\partial a_{f_i}}$ is $\psi_i \in \mathbb{R}$.

The geometric parameters including the metric tensor, curvature tensor, and torsion tensor are used to define the rolling contact kinematics. For ease of notation, $\boldsymbol{c}_a, \boldsymbol{c}_b$ respectively denote $\frac{\partial \boldsymbol{c}_{f_i}}{\partial a_{f_i}}$ and $\frac{\partial \boldsymbol{c}_{f_i}}{\partial b_{f_i}}$. The Gauss frame is used to define the contact frame $\mathcal{C}_i$:

$$R_{fc_i} = \begin{bmatrix} \boldsymbol{r}_x & \boldsymbol{r}_y & \boldsymbol{r}_z \end{bmatrix} = \begin{bmatrix} \frac{\boldsymbol{c}_a}{||\boldsymbol{c}_a||} & \frac{\boldsymbol{c}_a}{||\boldsymbol{c}_b||} & \boldsymbol{n} \end{bmatrix} \tag{5}$$

where $R_{fc_i} \in SO(3)$ maps $\mathcal{C}_i$ to $\mathcal{F}_i$ and

$$\boldsymbol{n} = \frac{\boldsymbol{c}_a \times \boldsymbol{c}_b}{||\boldsymbol{c}_a \times \boldsymbol{c}_b||} \tag{6}$$

The metric tensor, $M_{f_i} := M_{f_i}(\boldsymbol{\xi}_{f_i}) \in \mathbb{R}^{2\times 2}$, curvature tensor, $K_{f_i} := K_{f_i}(\boldsymbol{\xi}_{f_i}) \in \mathbb{R}^{2\times 2}$, and torsion tensor, $T_{f_i} := T_{f_i}(\boldsymbol{\xi}_{f_i}) \in \mathbb{R}^{2\times 2}$ are defined by:

$$M_{f_i} = \begin{bmatrix} ||\boldsymbol{c}_a|| & 0 \\ 0 & ||\boldsymbol{c}_b|| \end{bmatrix} \tag{7}$$

$$K_{f_i} = \begin{bmatrix} \boldsymbol{r}_x^T \\ \boldsymbol{r}_y^T \end{bmatrix} \begin{bmatrix} \frac{\partial \boldsymbol{n}/\partial a}{||\boldsymbol{c}_a||} & \frac{\partial \boldsymbol{n}/\partial b}{||\boldsymbol{c}_b||} \end{bmatrix} \tag{8}$$

$$T_{f_i} = \boldsymbol{r}_y^T \begin{bmatrix} \frac{\partial \boldsymbol{r}_a/\partial a}{||\boldsymbol{c}_a||} & \frac{\partial \boldsymbol{r}_x/\partial b}{||\boldsymbol{c}_b||} \end{bmatrix} \tag{9}$$

Note the same geometric parameters can be defined for the object contact points by substituting $\boldsymbol{\xi}_{f_i}$ with $\boldsymbol{\xi}_{o_i}$ in (5)-(9). Now we can define the dynamics governing the contact parameters $\boldsymbol{\xi}_f$ by:

$$\dot{\boldsymbol{\xi}}_{f_i} = HR_{c_ip}(\boldsymbol{\omega}_{f_i} - \boldsymbol{\omega}_o) \tag{10}$$

where

$$H = M_{f_i}^{-1}(K_{f_i} + R_{\psi_i}K_{o_i}R_{\psi_i})^{-1}\begin{bmatrix} 0 & -1 & 0 \\ 1 & 0 & 0 \end{bmatrix}, \tag{11}$$

$$R_{\psi_i} = \begin{bmatrix} \cos(\psi_i) & -\sin(\psi_i) \\ -\sin(\psi_i) & -\cos(\psi_i) \end{bmatrix}, \tag{12}$$

$$\dot{\psi}_i = T_{f_i}M_{f_i}\dot{\boldsymbol{\xi}}_{f_i} + T_{o_i}M_{o_i}\dot{\boldsymbol{\xi}}_{o_i} \tag{13}$$

$R_{c_ip} := R_{c_ip}(\boldsymbol{\xi}_{f_i}, \boldsymbol{q}_i) \in \mathbb{SO}(3)$ maps $\mathcal{P}$ to $\mathcal{C}_i$, and $M_{o_i}, K_{o_i}, T_{o_i}$ are the respective metric, curvature, and torsion tensors for the object contact i.

The chosen parameterizations must satisfy [8]:

Assumption 4. *The parameterizations are orthogonal such that* $\frac{\partial \boldsymbol{c}_{f_i}}{\partial a_{f_i}}^T \frac{\partial \boldsymbol{c}_{f_i}}{\partial b_{f_i}} = 0$, $\frac{\partial \boldsymbol{c}_{o_i}}{\partial a_{o_i}}^T \frac{\partial \boldsymbol{c}_{o_i}}{\partial b_{o_i}} = 0$, *and* $M_{f_i}, K_{f_i}, T_{f_i}, M_{o_i}, K_{o_i}, T_{o_i}$ *are defined for all* $\boldsymbol{\xi}_{f_i}$ *on the fingertip surface, and* $\boldsymbol{\xi}_{o_i}$ *on the object surface, respectively.*

III. Zeroing Control Barrier Functions for Relative Degree Two Systems

Control barrier functions provide a formal method to ensure constraint satisfaction of dynamical systems. Zeroing control barrier functions is a subset of control barrier functions, which are known to be robust to modeling errors and conducive to real-time applications [17]. Here we extend the existing work of [17] to relative degree two systems for application in robotic grasping and manipulation.

Consider the following nonlinear affine system:

$$\ddot{\boldsymbol{x}} = \boldsymbol{f}(\boldsymbol{x}, \dot{\boldsymbol{x}}) + \boldsymbol{g}(\boldsymbol{x}, \dot{\boldsymbol{x}})\boldsymbol{u} \tag{14}$$

where $\boldsymbol{x} \in \mathbb{R}^p$ is the system state, $\boldsymbol{u} \in U \subseteq \mathbb{R}^m$ is the control input, and $\boldsymbol{f}, \boldsymbol{g}$ are locally Lipschitz continuous functions that define the system dynamics. The goal of constraint satisfaction is to ensure the states $\boldsymbol{x}$ stay within a set of constraint-admissable states defined by:

$$\mathcal{D} = \{\boldsymbol{x} \in \mathbb{R}^p : h(\boldsymbol{x}) \geq 0\} \tag{15}$$

where $h : \mathbb{R}^p \to \mathbb{R}$ is a continuously differentiable function of relative degree two.

Definition 1. *A continuous function,* $\alpha : (-b, a) \to (-\infty, \infty)$ *for* $a, b \in \mathbb{R}_{>0}$ *is an extended class-*$\mathcal{K}$ *function if it is strictly increasing and* $\alpha(0) = 0$.

Let $B : \mathbb{R}^p \times \mathbb{R}^p \to \mathbb{R}$ be defined by:

$$B(\boldsymbol{x}, \dot{\boldsymbol{x}}) = \frac{\partial h}{\partial \boldsymbol{x}}\dot{\boldsymbol{x}} + \alpha_1(h(\boldsymbol{x})) \tag{16}$$

where α_1 is an extended class-$\mathcal{K}$ function. Let the set $\mathcal{E}$ be defined by:

$$\mathcal{E} = (\mathcal{D} \times \mathbb{R}^p) \bigcap \{(\boldsymbol{x}, \dot{\boldsymbol{x}}) \in \mathbb{R}^p \times \mathbb{R}^p : B(\boldsymbol{x}, \dot{\boldsymbol{x}}) \geq 0\} \tag{17}$$

Definition 2. *Let* h *by a continuously differentiable, relative degree two function for the system* (14). *A continuously differentiable function* $B : \mathbb{R}^p \times \mathbb{R}^p \to \mathbb{R}$ *defined by* (16)*, is a zeroing control barrier function for the set* $\mathcal{E}$ *if there exists an extended class-*$\mathcal{K}$ *function* α_2 *such that for all* $(\boldsymbol{x}, \dot{\boldsymbol{x}}) \in \mathcal{E}$,

$$\sup_{\boldsymbol{u} \in U}\{L_fB + L_gB\boldsymbol{u} + \alpha_2(B) \geq 0\} \tag{18}$$

Given a zeroing control barrier function B, for all $(\boldsymbol{x}, \dot{\boldsymbol{x}}) \in \mathcal{E}$ define the set:

$$S_u(\boldsymbol{x}, \dot{\boldsymbol{x}}) = \{\boldsymbol{u} \in U : L_fB + L_gB\boldsymbol{u} + \alpha_2(B) \geq 0\} \tag{19}$$

Constraint satisfaction using zeroing control barrier functions is ensured by the following theorem:

Theorem 1. *Given sets* $\mathcal{D}, \mathcal{E}$ *defined by* (15), (17) *respectively, for a continuously differentiable, relative degree two function* h*, if* $(\boldsymbol{x}(0), \dot{\boldsymbol{x}}(0)) \in \mathcal{E}$ *and* B *is a zeroing control barrier function, then for any Lipschitz control* $\boldsymbol{u} : \mathcal{E} \to U$ *such that* $\boldsymbol{u}(\boldsymbol{x}, \dot{\boldsymbol{x}}) \in S_u(\boldsymbol{x}, \dot{\boldsymbol{x}})$ *for the system* (14)*,* $\boldsymbol{x}$ *remains in* $\mathcal{D}$ *for all* $t > 0$.

Proof. For $(\boldsymbol{x}(0), \dot{\boldsymbol{x}}(0)) \in \mathcal{E}$, and $\boldsymbol{u} \in S_u$, it follows from Corollary 2 of [17] that the set $\{(\boldsymbol{x}, \dot{\boldsymbol{x}}) \in \mathbb{R}^p \times \mathbb{R}^p : B(\boldsymbol{x}, \dot{\boldsymbol{x}}) \geq 0\}$ is forward invariant. Thus $B \geq 0$ holds for a given extended class-$\mathcal{K}$ function α_1. It follows that h is a zeroing barrier function according to Definition 3 of [17]. Thus by Proposition 1 of [17], $\mathcal{D}$ is forward invariant. ☐

Remark 2. *The use of the two staggered extended class-*$\mathcal{K}$ *functions in Theorem 1 allows a designer to adjust the performance of the control barrier functions for more aggressive or conservative constraint satisfaction. Note that for general nonlinear systems the condition that* $(\boldsymbol{x}(0), \dot{\boldsymbol{x}}(0)) \in \mathcal{E}$ *may be restrictive, however in-hand manipulation tasks generally begin from a static grasp, such that satisfaction of* $(\boldsymbol{x}(0), 0) \in \mathcal{E}$ *is trivial. However the condition does allow for more aggressive initial grasps such as if, for example, the hand catches the object prior to a manipulation task.*

IV. Proposed Solution

In the following section, the set of constraint admissible grasp states is defined, and the zeroing control barrier function approach developed from Section III is applied to derive the grasp constraints. The grasp constraints are then combined to define the proposed controller.

A. Constraint-Admissible Grasping States

Satisfaction of the following condition ensures the object will not slip within the grasp [5]:

$$\Lambda(\mu)R_{cp}\boldsymbol{f}_c > 0 \tag{20}$$

where $\mu \in \mathbb{R}_{>0}$ is the friction coefficient, $\Lambda(\mu) \in \mathbb{R}^{l_s \times 3n}$ is a polyhedral of $l_s \in \mathbb{Z}_{>0}$ faces used to a approximate the friction cone [7], and $R_{cp} \in \mathbb{R}^{3n \times 3n}$ is the block diagonal matrix of all R_{c_ip} for $i \in [1, n]$. Let the set of constraint admissible contact forces be defined as:

$$\mathcal{D}_f = \{\boldsymbol{f}_c \in \mathbb{R}^{3n} : \Lambda(\mu)R_{cp}\boldsymbol{f}_c > 0\} \tag{21}$$

Let the set of admissible joint angles be defined by:

$$\begin{aligned} h_{q\max_j}(\boldsymbol{q}) &= -\boldsymbol{e}_j\boldsymbol{q} + q_{\max_j} \geq 0, \forall j \in [1, m] \\ h_{q\min_j}(\boldsymbol{q}) &= \boldsymbol{e}_j\boldsymbol{q} - q_{\min_j} \geq 0, \forall j \in [1, m] \end{aligned} \tag{22}$$

where $e_j \in \mathbb{R}^{1\times m}$ is the jth row of $I_{m\times m}$ and $q_{\max_j}, q_{\min_j} \in \mathbb{R}_{\geq 0}$ define the joint angle limits, which omit singular hand configurations. The set of constraint admissible joint angles is defined by:

$$\mathcal{D}_q = \{\boldsymbol{q} \in \mathbb{R}^m : h_{q\max}(\boldsymbol{q}) \geq 0, h_{q\min}(\boldsymbol{q}) \geq 0\} \quad (23)$$

The fingertip workspace is addressed here via the geometric modeling of the contact kinematics. Many existing tactile sensors are designed as flat or hemispherical fingertips [10], which can be appropriately modeled with geometric parameterizations [8]. The benefit of the geometric modeling is not only that it can be applied to general fingertip shapes, but the fingertip workspace can be defined as simple box constraints:

$$\begin{aligned} h_1(\boldsymbol{\xi}_{f_i}) &= \begin{bmatrix} 1 & 0 \end{bmatrix} \boldsymbol{\xi}_{f_i} - a_{\min} \\ h_2(\boldsymbol{\xi}_{f_i}) &= -\begin{bmatrix} 1 & 0 \end{bmatrix} \boldsymbol{\xi}_{f_i} + a_{\max} \\ h_3(\boldsymbol{\xi}_{f_i}) &= \begin{bmatrix} 0 & 1 \end{bmatrix} \boldsymbol{\xi}_{f_i} - b_{\min} \\ h_4(\boldsymbol{\xi}_{f_i}) &= -\begin{bmatrix} 0 & 1 \end{bmatrix} \boldsymbol{\xi}_{f_i} + b_{\max} \end{aligned} \quad (24)$$

where $a_{\min}, a_{\max}, b_{\min}, b_{\max} \in \mathbb{R}_{\geq 0}$ define the fingertip surface, and each h_j define the box constraints such that if $h_j \geq 0, \forall j \in [1,4]$, the contact point is in the fingertip workspace. The set of allowable contact locations is $\mathcal{D}_r = \mathcal{D}_{r_1} \times \ldots \times \mathcal{D}_{r_n}$ for:

$$\mathcal{D}_{r_i} = \{\boldsymbol{\xi}_{f_i} \in \mathbb{R}^2 : h_j(\boldsymbol{\xi}_{f_i}) \geq 0, \forall j \in [1,4]\} \quad (25)$$

Let $\mathcal{H} = \mathcal{D}_f \times \mathcal{D}_q \times \mathcal{D}_r$ denote the set of grasp constraint admissible states. In the set $\mathcal{H}$, the hand configuration is non-singular and thus by Assumption 1 J_h is invertible. Furthermore, the contact points do not slip in $\mathcal{H}$ and so the grasp constraint (4) holds. Differentiation of (4), and and substitution of (1) and (2) provides an expression for the contact forces as a function of the control torque, $\boldsymbol{u}$:

$$\boldsymbol{f}_c = \left(J_h M_h^{-1} J_h^T + G M_o^{-1} G^T\right)^{-1} \Big(J_h M_h^{-1}(-C_h \dot{\boldsymbol{q}} + \boldsymbol{u} + \boldsymbol{\tau}_e) + \dot{J}_h \dot{\boldsymbol{q}} - \frac{d}{dt}[G^T]\dot{\boldsymbol{x}}_o + G^T M_o^{-1}(C_o \dot{\boldsymbol{x}}_o - \boldsymbol{w}_e) \quad (26)$$

Note that by Assumptions 1 and 2, the inversion of $J_h M_h^{-1} J_h^T + G M_o^{-1} G^T$ is well defined.

B. Proposed Controller

The following constraints are developed to ensure forward invariance of $\mathcal{H}$ with respect to the states $(\boldsymbol{f}_c, \boldsymbol{q}, \boldsymbol{\xi}_f)$.

The no slip constraint is defined by (26) into (20) [5]:

$$\Lambda(\mu) R_{cp} B_{ho}^{-1} J_h M_h^{-1} \boldsymbol{u} > \Lambda(\mu) R_{cp} B_{ho}^{-1} J_h M_h^{-1}(C_h \dot{\boldsymbol{q}} - \boldsymbol{\tau}_e) - \dot{J}_h \dot{\boldsymbol{q}} + \frac{d}{dt}[G^T]\dot{\boldsymbol{x}}_o - G^T M_o^{-1}(C_o \dot{\boldsymbol{x}}_o - \boldsymbol{w}_e) \quad (27)$$

where $B_{ho} = (J_h M_h^{-1} J_h^T + G M_o^{-1} G^T)$. Satisfaction of (27) by $\boldsymbol{u}$ directly ensures forward invariance of $\mathcal{D}_f$. Note that by Assumption 1, (27) is defined for all states in $\mathcal{H}$.

The zeroing control barrier functions from Section III are used here to guarantee that the hand joints remain inside a desired joint space to prevent over-extension. Let the zeroing control barrier functions be defined by:

$$\begin{aligned} B_{q\max_j}(\boldsymbol{q}, \dot{\boldsymbol{q}}) &= \dot{h}_{q\max_j} + \alpha_1(h_{q\max_j}), \forall j \in [1,m] \\ B_{q\min_j}(\boldsymbol{q}, \dot{\boldsymbol{q}}) &= \dot{h}_{q\min_j} + \alpha_1(h_{q\min_j}), \forall j \in [1,m] \end{aligned} \quad (28)$$

where $\alpha_1(h)$ is an extended class-$\mathcal{K}$ function. Let $\mathcal{E}_q$ be defined by:

$$\mathcal{E}_q = (\mathcal{D}_q \times \mathbb{R}^m) \bigcap \{(\boldsymbol{q}, \dot{\boldsymbol{q}}) \in \mathbb{R}^m \times \mathbb{R}^m : B_{q\max_j} \geq 0, B_{q\min_j} \geq 0, \forall j \in [1,m]\} \quad (29)$$

Following Theorem 1 and by using the dynamics (1) and contact force relation (26), if the control torque satisfies the following constraint for a given $\alpha_2(h)$ extended class-$\mathcal{K}$ function, then $\mathcal{D}_q$ is rendered forward invariant:

$$A_q \boldsymbol{u} \geq \boldsymbol{b}_q \quad (30)$$

where $A_q \in \mathbb{R}^{2m\times m}$ and $\boldsymbol{b}_q \in \mathbb{R}^{2m}$ are the respective concatenations of $L_g B_{q\max_j}, L_g B_{q\min_j}, j \in [1,m]$ and $-L_f B_{q\max_j} - \alpha_2(B_{q\max_j}), -L_f B_{q\min_j} - \alpha_2(B_{q\min_j}) \forall j \in [1,m]$. Let the set of admissable control torques for $\mathcal{D}_q$ be $S_{u_q} = \{\boldsymbol{u} \in \mathbb{R}^m : A_q \boldsymbol{u} \geq \boldsymbol{b}_q\}$.

The zeroing control barrier functions are also used to ensure the contact points remain in the fingertip workspace. We define the candidate zeroing control barrier functions:

$$B_{r_j}(\boldsymbol{\xi}_{f_i}, \dot{\boldsymbol{\xi}}_{f_i}) = \dot{h}_j(\boldsymbol{\xi}_{f_i}) + \alpha_1(h_j(\boldsymbol{\xi}_{f_i})),\ \forall j \in [1,4] \quad (31)$$

with associated set $\mathcal{E}_r = \mathcal{E}_{r_1} \times \ldots \times \mathcal{E}_{r_n}$ where

$$\mathcal{E}_{r_i} = (\mathcal{D}_{r_i} \times \mathbb{R}^4) \bigcap \{(\boldsymbol{\xi}_{f_i}, \dot{\boldsymbol{\xi}}_{f_i}) \in \mathbb{R}^4 : B_{r_j}(\boldsymbol{\xi}_{f_i}, \dot{\boldsymbol{\xi}}_{f_i}) \geq 0, \forall j \in [1,4]\} \quad (32)$$

Following the approach from Theorem 1, the following condition must be satisfied to ensure forward invariance of $\mathcal{E}_r$:

$$L_f B_j + L_g B_j \boldsymbol{u}_i + \alpha_2(B_j) \geq 0,\ \forall j \in [1,4], \forall i \in [1,n] \quad (33)$$

By Assumption 3, the terms $L_f B_j, L_g B_j$ are derived by differentiating (10) as follows:

$$\ddot{\boldsymbol{\xi}}_{f_i} = \frac{d}{dt}\Big[H_i R_{g_i p}\Big](\boldsymbol{\omega}_{f_i} - \boldsymbol{\omega}_o) + H_i R_{g_i p} \begin{bmatrix} 0_{3\times3} & I_{3\times3} \end{bmatrix} \Big(\dot{J}_{s_i} \dot{\boldsymbol{q}}_i + J_{s_i} \ddot{\boldsymbol{q}}_i - \ddot{\boldsymbol{x}}_o\Big) \quad (34)$$

Substitution of (1), (2), and (26) into (34), provides the necessary derivation of $L_f B_j, L_g B_j$.

Re-writing (33), if the control torque satisfies the following constraint, then $\mathcal{D}_r$ is forward invariant:

$$A_r \boldsymbol{u} \geq \boldsymbol{b}_r \quad (35)$$

where $A_r \in \mathbb{R}^{4k\times m}$ and $\boldsymbol{b}_r \in \mathbb{R}^{4k}$ are the respective columnwise concatenation over the n contact points of:

$$A_{r_i} = \begin{bmatrix} L_g B_1(\boldsymbol{\xi}_{f_i}, \dot{\boldsymbol{\xi}}_{f_i}) \\ \ldots \\ L_g B_4(\boldsymbol{\xi}_{f_i}, \dot{\boldsymbol{\xi}}_{f_i}) \end{bmatrix} \quad (36)$$

$$\boldsymbol{b}_{r_i} = \begin{bmatrix} -L_f B_1(\boldsymbol{\xi}_{f_i}, \dot{\boldsymbol{\xi}}_{f_i}) - \alpha_2(B_1(\boldsymbol{\xi}_{f_i}, \dot{\boldsymbol{\xi}}_{f_i})) \\ \dots \\ -L_f B_4(\boldsymbol{\xi}_{f_i}, \dot{\boldsymbol{\xi}}_{f_i}) - \alpha_2(B_4(\boldsymbol{\xi}_{f_i}, \dot{\boldsymbol{\xi}}_{f_i})) \end{bmatrix} \tag{37}$$

Let the set of admissible control torques be $S_{u_r} = \{\boldsymbol{u} \in \mathbb{R}^m : A_r \boldsymbol{u} \geq \boldsymbol{b}_r\}$.

Finally, actuators are limited to a finite actuation range in real-life applications. To ensure the proposed controller is implementable on real systems the following actuator constraint is defined:

$$\boldsymbol{u}_{\text{min}} \leq \boldsymbol{u} \leq \boldsymbol{u}_{\text{max}} \tag{38}$$

Let the set of grasp constraint admissible control torques be $S_u = S_{u_f} \times S_{u_q} \times S_{u_r} \times \{\boldsymbol{u} \in \mathbb{R}^m : \boldsymbol{u}_{\text{min}} \leq \boldsymbol{u} \leq \boldsymbol{u}_{\text{max}}\}$.

Assumption 5. *The set of grasp constraint admissible control torques S_u is non-empty.*

Motivated by the notion of safety-critical control [17], we propose a novel controller that admits a nominal manipulation controller, $\boldsymbol{u}_{\text{nom}} \in \mathbb{R}^m$, and outputs a control torque that stays minimally close to $\boldsymbol{u}_{\text{nom}}$, in the 2-norm sense, while adhering to the grasp constraints. The proposed control law is:

$$\begin{aligned} \boldsymbol{u}^* &= \underset{\boldsymbol{u}}{\text{argmin}}\ (\boldsymbol{u} - \boldsymbol{u}_{\text{nom}})^T (\boldsymbol{u} - \boldsymbol{u}_{\text{nom}}) \\ &\text{s.t.} \qquad (27), (30), (35), (38) \end{aligned} \tag{39}$$

Proposition 1. *Suppose Assumptions 1-5 hold and $\boldsymbol{f}_c(0) \in \mathcal{D}_f$, $(\boldsymbol{q}(0), \dot{\boldsymbol{q}}(0)) \in \mathcal{E}_q$, $\boldsymbol{\xi}_f(0), \dot{\boldsymbol{\xi}}_f(0)) \in \mathcal{E}_r$. If $\boldsymbol{u}_{nom} \in \mathbb{R}^m$ is Lipschitz, then* (39) *applied to* (1) *ensures $\mathcal{H}$ is forward invariant.*

V. Results

Here we present numerical simulations in which we compare a nominal manipulation controller from the literature with the same controller implemented via the proposed controller (39). The controllers are implemented as if in a hierarchical grasp framework where a reference command is provided to the robotic hand from a high-level planner. The nominal controller is the computed torque control [8], [16] along with a conventional internal force control [4] of the form:

$$\boldsymbol{u}_{\text{nom}} = J_h^T (G^\dagger \boldsymbol{u}_m + \boldsymbol{u}_f) - \boldsymbol{\tau}_e \tag{40}$$

$$\boldsymbol{u}_m = M_{ho} P(\ddot{\boldsymbol{r}} + K_p \boldsymbol{e} + K_d \dot{\boldsymbol{e}}) + C_{ho} \dot{\boldsymbol{x}}_o - \boldsymbol{w}_e \tag{41}$$

$$\boldsymbol{u}_f = k_f (\bar{\boldsymbol{p}}_c - \boldsymbol{p}_{c_1}, \bar{\boldsymbol{p}}_c - \boldsymbol{p}_{c_2}, ..., \bar{\boldsymbol{p}}_c - \boldsymbol{p}_{c_n}) \tag{42}$$

where where $G^\dagger = G^T(GG^T)^{-1}$, $\boldsymbol{e} \in \mathbb{R}^6$ is the error between the reference and object pose defined using Euler angles as in [16], $P \in \mathbb{R}^{6\times 6}$ maps the object velocity using Euler angles to $\dot{\boldsymbol{x}}_o$ [16], $M_{ho} = M_o + GJ_h^{-T} M_h J_h^{-1} G^T$, $C_{ho} = C_o + GJ_h^{-T}(C_h J_h^{-1} G^T + M_h \frac{d}{dt}[J_h^{-1} G^T])$, $K_p, K_d \in \mathbb{R}^{6\times 6}$ are the respective proportional and derivative positive definite control gains, $\boldsymbol{r} \in \mathbb{R}^6$ is the reference command, $\bar{\boldsymbol{p}}_c = \frac{1}{n}\sum_{i=1}^n \boldsymbol{p}_{c_i}$ is the centroid of the inertial contact positions, and $k_f \in \mathbb{R}_{>0}$ is a squeezing scalar gain. The gains chosen for the simulation are $K_p = 1.0 * I_{6\times 6}$, $K_d = 2.5 * I_{6\times 6}$, $k_f = 10.0$.

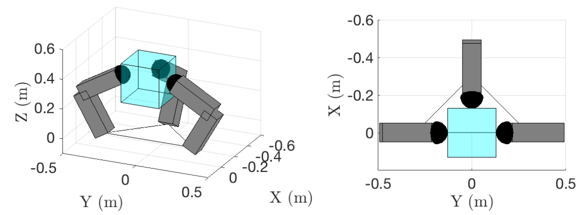

(a) Isometric view. (b) Top view.

Fig. 2: Simulation setup.

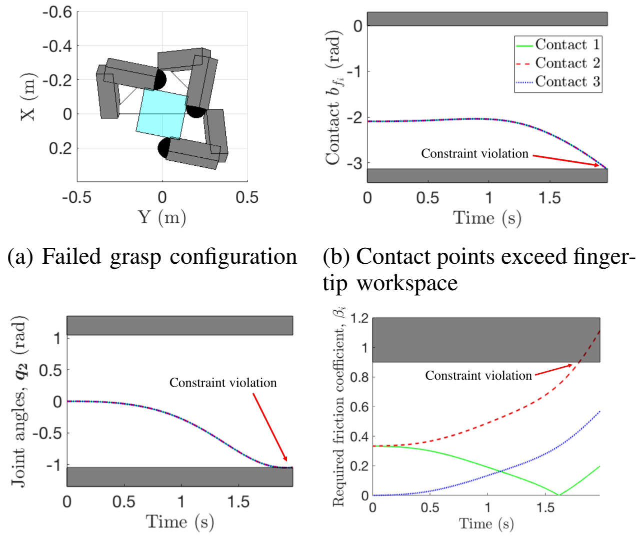

(a) Failed grasp configuration (b) Contact points exceed fingertip workspace

(c) Joint limits exceeded (d) Slip constraint violated

Fig. 3: Nominal controller.

The reference $\boldsymbol{r} = (0, 0, 0.25\cos(t), 0, 0, 2\cos(t))$ is provided to twist and pull the object about the Z-axis of the inertial frame, which is depicted in Figure 2 along with the initial static hand-object configuration. The grasped object is a 0.11 kg cube with edge length of 0.2604 m. The friction coefficient between the object and fingertip is $\mu = 0.9$. The hand is composed of identical rectangular prismatic links of dimension $0.3 \times 0.05 \times 0.05$ m^3 with hemispherical fingertips of radius $R = 0.06$ m. Each finger consists of 2 revolute joints at the base and one between the two links. The fingertip parameterization chosen to satisfy Assumption 4 is $\boldsymbol{c}_{f_i} = [-R\cos(a_{f_i})\cos(b_{f_i}), R\sin(a_{f_i}), -R\cos(a_{f_i})\sin(b_{f_i})]^T$. The associated box constraints to define the fingertip workspace are: $-\pi/2 < a_{f_i} < \pi/2$, $-\pi < b_{f_i} < 0$. The joint angle limits for each finger are $\boldsymbol{q}_{\text{max}_i} = (3\pi/2, \pi/3, 3\pi/2)$, $\boldsymbol{q}_{\text{min}_i} = (0, -\pi/3, 0)$, $\forall i \in [1, 3]$. The extended class-$\mathcal{K}$ functions used in the control barrier functions of (39) are $\alpha_1(h) = \alpha_2(h) = h^3$. Note the only disturbance acting on the system is gravity. The simulations were performed using Matlab's ode3 integrator. The simulation time was 15 seconds, but simulations were stopped if the contact points exceed the fingertip workspace.

The implementation of the nominal control resulted in a failed grasp as shown in Figure 3. The gray regions denote

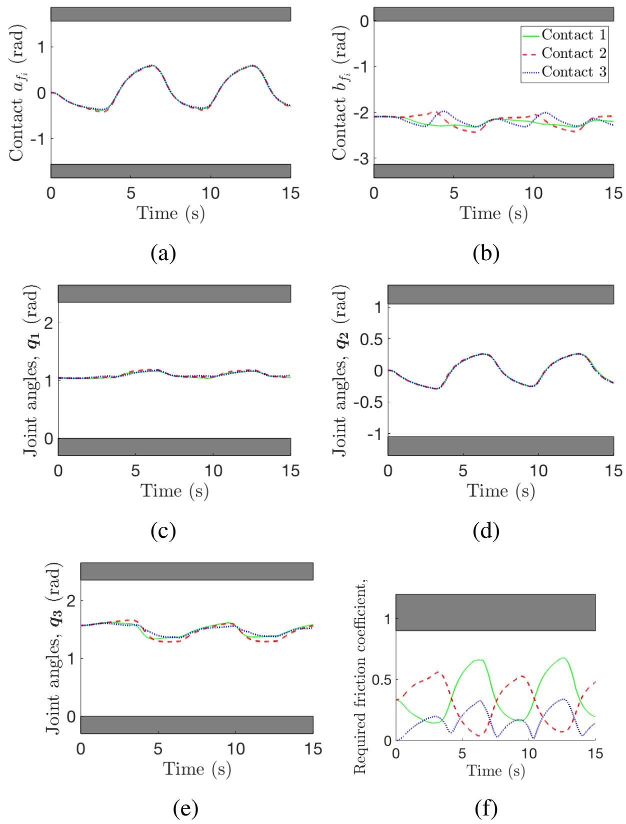

Fig. 4: Grasping states for proposed controller.

areas outside of the constraint admissible state space. Figure 3b shows that as the nominal control rotates the object to track the reference pose, all of the contact trajectories, b_{f_i}, exceed the fingertip workspace resulting in loss of contact. Figure 3c shows that the joint angles also exceed the prescribed joint limits. Figure 3d shows the required friction, $\beta_i \in \mathbb{R}_{>0}$, which denotes the friction required at each contact to perform the manipulation motion [5]. If the required friction β_i exceeds the friction coefficient μ, then the contact points slip, which is depicted in Figure 3d. Thus the reference provided by the high-level grasp planner is infeasible for the nominal control.

Figure 4 shows the grasp states from the proposed control (39), which admits the nominal control (40). Figures 4a and 4b show the contact trajectories remain inside the fingertip workspace. Figures 4c-4e show that the joint angles also remain within the defined joint angle limits. Figure 4f shows the required friction, β_i, remains below the slipping region. The combined satisfaction of all grasp constraints validates the forward invariance of the grasp constraint admissible set $\mathcal{H}$ as per Proposition 1. We note that appropriate choice of α_1 and α_2 allows for more aggressive/conservative controller performance. These results show that the proposed controller prevents grasp failure even when the high-level planner provides an infeasible reference command for the given nominal control.

The numerical simulations show promising results for ensuring grasp constraint satisfaction during in-hand manipulation. However the proposed controller (39) is only defined if Assumption 5 holds. Future work will investigate feasibility conditions regarding Assumption 5.

VI. Conclusion

In this paper, a control law was proposed to guarantee grasp constraint satisfaction for in-hand manipulation using robotic hands. The grasp constraints were derived to ensure the object does not slip, the joints do not exceed joint angle limits, and the contact points do not leave the fingertip workspace. The proposed controller admits an existing nominal manipulation control, while adhering to the grasp constraints to support the assumptions made in the literature. Numerical results demonstrate the efficacy of the proposed approach.

References

[1] A. Bicchi, "Hands for dexterous manipulation and robust grasping: A difficult road toward simplicity," *IEEE Trans. Robot. Autom.*, vol. 16, no. 6, pp. 652–662, 2000.

[2] K. Hang, M. Li, J. Stork, Y. Bekiroglu, F. Pokorny, A. Billard, and D. Kragic, "Hierarchical fingertip space: A unified framework for grasp planning and in-hand grasp adaptation," *IEEE Trans. Robot.*, vol. 32, no. 4, pp. 960–972, 2016.

[3] V. Lippiello, F. Ruggiero, B. Siciliano, and L. Villani, "Visual grasp planning for unknown objects using a multifingered robotic hand," *IEEE/ASME Trans. Mechatronics*, vol. 18, no. 3, pp. 1050–1059, 2013.

[4] R. Ozawa and K. Tahara, "Grasp and dexterous manipulation of multi-fingered robotic hands: A review from a control view point," *Adv. Robotics*, vol. 31, pp. 1030–1050, 2017.

[5] W. Shaw-Cortez, D. Oetomo, C. Manzie, and P. Choong, "Tactile-based blind grasping: A discrete-time object manipulation controller for robotic hands," *IEEE Robot. Autom. Lett.*, vol. 3, no. 2, 2018.

[6] A. Caldas, A. Micaelli, M. Grossard, M. Makarov, P. Rodriguez-Ayerbe, and D. Dumur, "Object-level impedance control for dexterous manipulation with contact uncertainties using an LMI-based approach," in *Proc. IEEE Int. Conf. Robot. Automat.*, 2015, pp. 3668–3674.

[7] M. Nahon and J. Angeles, "Real-time force optimization in parallel kinematic chains under inequality constraints," *IEEE Trans. Robot. Autom.*, vol. 8, no. 4, pp. 439–450, 1992.

[8] R. Murray, Z. Li, and S. Sastry, *A mathematical introduction to robotic manipulation*. CRC Press: Boca Raton, FL, USA, 1994.

[9] D. Montana, "The kinematics of contact and grasp," *Int. J. Robot. Res.*, vol. 7, no. 3, pp. 17–32, 1988.

[10] Z. Kappassov, J. Corrales, and V. Perdereau, "Tactile sensing in dexterous robot hands - review," *Robot. Auton. Syst.*, vol. 74, pp. 195–220, 2015.

[11] A. Kawamura, K. Tahara, R. Kurazume, and T. Hasegawa, "Dynamic grasping of an arbitrary polyhedral object," *Robotica*, vol. 31, no. 4, pp. 511–523, 2013.

[12] T. Wimböck, C. Ott, A. Albu-Schäffer, and G. Hirzinger, "Comparison of object-level grasp controllers for dynamic dexterous manipulation," *Int. J. Robot. Res.*, vol. 31, no. 1, pp. 3–23, 2012.

[13] K. Hertkorn, M. Roa, and C. Borst, "Planning in-hand object manipulation with multifingered hands considering task constraints," in *Proc. IEEE Int. Conf. Robot. Automat.*, 2013, pp. 617–624.

[14] L. Han, Z. Li, J. Trinkle, Z. Qin, and S. Jiang, "The planning and control of robot dextrous manipulation," in *Proc. IEEE Int. Conf. Robot. Automat.*, vol. 1, 2000, pp. 263–269.

[15] M. Cherif and K. Gupta, "Planning quasi-static fingertip manipulations for reconfiguring objects," *IEEE Trans. Robot. Autom.*, vol. 15, no. 5, pp. 837–848, 1999.

[16] A. Cole, J. Hauser, and S. Sastry, "Kinematics and control of multifingered hands with rolling contact," *IEEE Trans. Autom. Control*, vol. 34, no. 4, pp. 398–404, 1989.

[17] A. Ames, X. Xu, J. Grizzle, and P. Tabuada, "Control barrier function based quadratic programs for safety critical systems," *IEEE Trans. Autom. Control*, vol. 62, no. 8, pp. 3861–3876, 2017.